Analysis for center deviation of circular target under perspective projection

Yu Sun
College of Computer Science and Technology, Xi'an University of Science and Technology, Xi'an, China

Received 28 September 2018
Revised 19 February 2019
31 March 2019
3 April 2019
Accepted 3 April 2019

Abstract

Purpose – Accurate feature localization is a fundamental problem in computer vision and visual measurement. In a perspective projection model of the camera, the projected center of a spatial circle and the center of the projection ellipse are not identical. This paper aims to show how to locate the real projection center precisely in the perspective projection of a space circle target.

Design/methodology/approach – By analyzing the center deviation caused by projection transformation, a novel method is presented to precisely locate the real projection center of a space circle using projective geometry. Solution distribution of the center deviation is analyzed, and the quadratic equation for determining the deviation is derived by locating vanishing points. Finally, the actual projected center of the circular target is achieved by solving the deviation quadratic equations.

Findings – The procedures of the author's method are simple and easy to implement. Experimental data calculated that maximum deviation occurs at approximately between $3\pi/10$ and $2\pi/5$ of the angle between the projection surface and the space target plane. The absolute reduction in error is about 0.03 pixels; hence, it is very significant for a high-accuracy solution of the position of the space circle target by minimizing systematic measurement error of the perspective projection.

Originality/value – The center deviation caused by the space circle projection transformation is analyzed, and the detailed algorithm steps to locate the real projection center precisely are described.

Keywords Feature extraction, Centre deviation, Circle, Perspective projection, Projective geometry

Paper type Research paper

1. Introduction

The mapping between three-dimensional (3D) and two-dimensional (2D) image coordinates is a basic requirement in 3D machine vision. It is also a critical step toward many practical robotic vision applications, including 3D modeling and vision measurement, photogrammetry and industrial metrology. Accurate feature localization acts as an input to many algorithms, including camera calibration and 3D reconstruction. Circular targets are preferably used for signalizing object points because of their easy identification, strong anti-noise ability and other characteristics (Heikkila, 2000; Heikkila and Silven, 1997; Ahn and Rüdiger, 1997). Circles are also very common shapes in many man-made objects. Perspective projection is generally not a shape-preserving transformation. Perspective projection distorts the shape of the circular features in the image plane depending on the angle and displacement between the object surface and the image plane. Only when the surface and the image plane are parallel, projections remain circular. However, targets often degenerate into

This work is supported by the Scientific and Technology Program funded by Xi'an City (Program 2017079CG/RC042(XAKD003)).

Engineering Computations
Vol. 36 No. 7, 2019
pp. 2403-2413

0264-4401
DOI 10.1108/EC-09-2018-0431

an ellipse in a circular projection transformation. So, the imaged center of a spatial circle and the center of the projection ellipse do not actually coincide. Therefore, center positioning errors exist. Coordinates of the center point of the mark are the most important input data; the accuracy of the positioning center has a direct effect on the measurement accuracy. Depending on the application, there are different requirements. In metrology applications, the precision is typically a more important factor. High geometrical accuracy is also needed in camera-based 3D measurements and in robot vision. Several factors limit the accuracy of feature localization among multiple views, including lens distortion, edge detection algorithm error, fitting algorithm error and perspective projection transforms distortion. Perspective projection transforms the center deviation, and this deviation error on the accuracy has been considered as a possible source of systematic measurement errors.

Much work has been done on the study of error compensation techniques for vision measurement systems (Huo *et al.*, 2018; Zhl *et al.*, 2011). Based on the 3D analytic geometry correction formula, Heikkila and Silven (1997) derived that centering deviation can be performed for each individual dot deviation correction. The difficulty lies in how to solve the landmark space relative to the camera posture. Heikkilae (2000) obtained by camera calibration matrix based on spatial attitude landmarks, but can only handle coplanar regularly distributed. The discrepancy between the ellipse centroid and the projection of the true feature point, computed in a different context by Ahnand Warnecke (1999), does not generalize to centroids computed from the center of mass in cases where the intensity distribution is nonuniform. The Hough transform needs point-by-point voting record and the use of more time, but accuracy is not high enough; although the least squares method can achieve sub-pixel accuracy, its anti-interference performance is poor, vulnerable to interference or noise point.

My approach is inspired by similar efforts to improve the accuracy by modeling sources of error at the feature extraction and localization phase. This paper is devoted to improving the precision of feature location of the space circular target. I propose a method of calculating the center deviation of the space circular target in the perspective projection transformation process and discuss the direction and characteristics of deviation.

2. Distribution of deviation

To analyze the deviation of two centers, the properties of an ellipse and perspective projection are used:

- The diameter parallel to the image plane is parallel to its projection in the image (CD//C′D′ in Figure 1).
- The center of an ellipse is on the connection obtained from midpoints of parallel chords (the center of the ellipse is on the A′B′ in Figure 1).
- The center of an ellipse bisects a chord through it (E′ is the midpoint of A′B′, that is the center of the ellipse in Figure 1).

Suppose for a set of circular object lines parallel to the image plane, then the lines in the circle plane are parallel to corresponding image lines. Thus, the midpoints of chords in the circle target are projected on the midpoints of chords in the ellipse. The midpoint O of diameter CD is perspective to the midpoint O′ of chord C′D′. The point O′ is the corresponding point of the circle center O. The line AB connecting the midpoints is projected to the A′B′ through the midpoints in C′D′. According to the properties of an ellipse, it is known that the midpoint of A′B′ is the ellipse center E′.

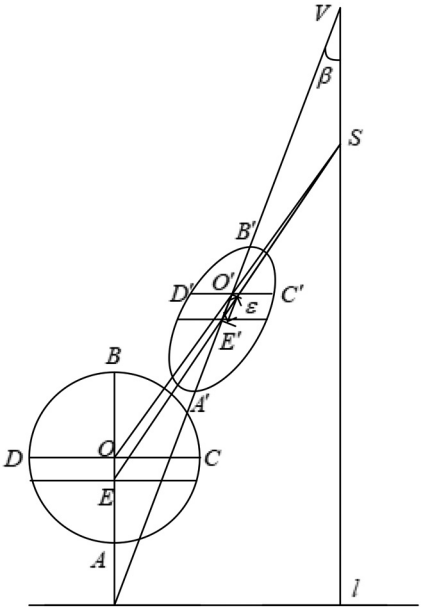

Figure 1.
Relation between circle center O and ellipse center E′

In the circular target plane, lines parallel to CD are parallel to the perspective axis. The connection AB with midpoints of the lines are perpendicular to the perspective axis. Therefore, the image point of the circle center and the ellipse center lies on the chord A′B′, that is to say the direction of the deviation of two centers in the image plane is pointed to the principal vanishing point V in Figure 1. The deviation between point O and point E departing from the principal vertical line with angle β is $1/\cos\beta$ times of the deviation ε between point O′ and point E′, which means that the deviation ε is in symmetrical distribution with the symmetry axis of the principal vertical line.

3. Deviation calculation

3.1 Calculation of deviation equation

The y-axis is chosen as the principal vertical line l and the x-axis is the principal horizontal line W, forming a right-handed coordinate system. The following terms are used in this paper and are illustrated in Figures 1 to 3

XYZ = World coordinate system;
$x^0y^0z^0$ = Horizontal image coordinate system;
xyz = Inclined image coordinate system;
uv = Image coordinate system associated with the xyz plane;
O = Center of the circular object target;
O′ = Corresponding image point of the circle center O;
E′ = Center of the image ellipse;
E = Corresponding object point in circle plane of the image ellipse center E';
α = Angle between the image plane and the circle plane;
β = Angle between the deviation and principal vertical line;
R = Radius of the circular object target;

f = focal length, principal distance;
H = vertical distance from camera to target plane;
V = principal vanishing point;
ni = mage nadir point; and
o = principal point of image.

In the image plane, the direction of the x-axis is chosen such that it is parallel to the intersection line between the image plane and the object target plane. The y-axis is perpendicular to the x-axis, forming the left-handed image coordinate system. The relationship between the image plane and the object plane is:

$$\begin{cases} x^0 = -f\left[x/(y\sin a - f\cos a)\right] \\ y^0 = -f\left[(y\cos a + f\sin a)/(y\sin a - f\cos a)\right] \end{cases} \tag{1}$$

Assuming the image coordinates of the ellipse center point E′ to be (0, v_e), here v_e = r, the deviation of the image point of the circular target center O′ and the ellipse center point E′ is ε, then the circular target center O (0, y_c^0) can be determined as:

$$y_c^0 = -f\frac{(v_e+\varepsilon)\cos\alpha + f\sin\alpha}{(v_e+\varepsilon)\sin\alpha - f\cos\alpha} \tag{2}$$

In the object coordinate system with the camera projection center as origin, H is the vertical distance from the camera to the target plane, and the target center O(0, Y_c) can be defined as:

$$Y_c = \frac{H}{f}\cdot y_c^0 = -H\frac{(v_e+\varepsilon)\cos\alpha + f\sin\alpha}{(v_e+\varepsilon)\sin\alpha - f\cos\alpha} \tag{3}$$

Given the target center O(0, Y_c), the circle diameter AB can be defined as A(0, Y_c−R), and B (0, Y_c + R). With equations (1) to (3), the intersection of the ellipse with the principal vertical line is A′B′, and its image coordinates are:

$$\begin{cases} v_b = \dfrac{A_1 f\cos\alpha + Bf\sin\alpha}{A_1\sin\alpha - B\cos\alpha} \\ v_a = \dfrac{A_2 f\cos\alpha + Bf\sin\alpha}{A_2\sin\alpha - B\cos\alpha} \end{cases} \tag{4}$$

Where

$$A_1 = A_{11} + A_{12}\varepsilon\,,\ A_{11} = H(r\cos\alpha + f\sin\alpha) + R(r\sin\alpha - f\cos\alpha),$$
$$A12 = (R\sin\alpha + H\cos\alpha)$$

$$A_2 = A_{21} + A_{22}\varepsilon, A_{21} = H(r\cos\alpha + f\sin\alpha) - R(r\sin\alpha - f\cos\alpha),$$
$$A22 = -(R\sin\alpha - H\cos\alpha)$$

$$B = B_1 + B_2\ \varepsilon,\quad B_1 = H(r\sin\alpha - f\cos\alpha)\ ,\ B_2 = H\sin\alpha$$

The relationship between v_a and v_b is:

$$(v_a + v_b)/2 = r \tag{5}$$

Inserting equation (4) into equation (5) leads to:

$$\frac{C_1 + C_2\varepsilon}{C_3 + C_4\varepsilon} + \frac{D_1 + D_2\varepsilon}{D_3 + D_4\varepsilon} = 2r \tag{6}$$

Where

$$C_1 = A_{11}fcos\alpha + B_1fsin\alpha,\ C_2 = A_{12}fcos\alpha + B_2fsin\alpha,\ C_3 = A_{11}sin\alpha - B_1fcos\alpha$$

$$C_4 = A_{12}fsin\alpha - B_2fcos\alpha,\ D_1 = A_{21}fcos\alpha + B_1fsin\alpha,\ D_2 = A_{22}fcos\alpha + B_1fsin\alpha$$

$$D_3 = A_{21}sin\alpha - B_1cos\alpha,\ D_4 = A_{22}sin\alpha - B_2cos\alpha.$$

Using equations (4) and (6):

$$(C_2D_4 + C_4D_2 - 2rC_4D_4)\varepsilon^2 + (C_1D_4 + C_2D_3 + C_4D_1 + C_3D_2 - 2rC_3D_4 - 2rC_4D_3)\varepsilon$$
$$+ C_1D_3 + C_3D_1 - 2rC_3D_3 = 0 \tag{7}$$

hence

$$2sin^3\alpha(rsin\alpha - fcos\alpha)\varepsilon^2 + \left(2H^2f^2/R^2 + 4\sin^2\alpha(r\sin\alpha - fcos\alpha)^2\right)\varepsilon$$
$$+ 2\sin\alpha(rsin\alpha - fcos\alpha)^3 = 0 \tag{8}$$

3.2 Analysis and selection of solutions

Given the general equation of deviation $ax^2 + bx + c = 0$, then the solution of the equation is:

$$\begin{cases} x_1 = \left(-b + \sqrt{b^2 - 4ac}\right)/2a \\ x_2 = \left(-b - \sqrt{b^2 - 4ac}\right)/2a & , a \neq 0 \\ x_1 = x_2 = 0, & a = 0 \end{cases}$$

The experiments show that x_1 with a μm grade value is an effective solution, and x_2 with hundreds of meters to several kilometers of the value is an invalid solution. In the following context, only deviation $\varepsilon = x_1$ is taken for discussion.

For perspective projection, the circle can be projected as an ellipse. In following discussion, the following are used: R for radius of the circular object target, f for principal distance and H for vertical distance from the camera to the target plane.

3.3 Verification of deviation equation

Three intermediate coordinate systems are selected in Figure 3.

Supposing that the image is taken as Figure 2 and the coordinates systems are selected as Figure 3, the deviation ε is pointing onto the principal vanishing point V; thus, ε is positive, and the angle α between the image plane and the circle plane is also positive. In Figure 2 supposing that $\overrightarrow{OW}$ is selected as the y-axis direction, in this case the direction of

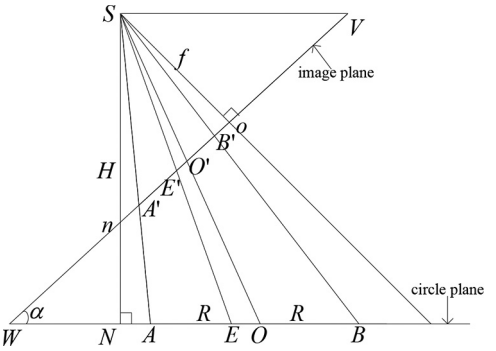

Figure 2.
Central projection of a circular target

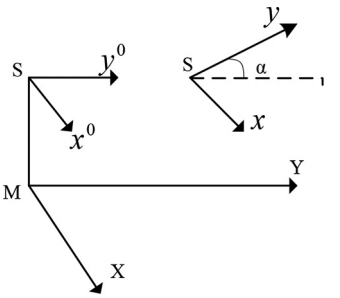

Figure 3.
Selection of the coordinate systems

rotation transformation α is clockwise, so α is negative. This means that any point e (0, r) on the principal vertical line with α positive and the point (0, −r) with α negative is the same point. In this case, the deviation value should be equal in magnitude, opposite in sign.

Let us assume that the parameters are taken as f = 8.0 mm, H = 1600.0 mm, R = 20 mm, $\alpha = \pm\pi/8$. As the image coordinates of the ellipse center point were (0, r), the parameter r varied from −20 mm to 20 mm during the experiment. The offsets ε are then solved in equation (8). The results are given in Table I.

For a given angle α shown in Figure 2, deviation should be gradually reduced from point W close to the principal vanishing point, until it reaches zero. The principal vanishing point V is as an imaging point at infinity of target, and therefore, there is no center deviation. Now $\alpha = \pi/3$ in Table II is discussed in detail. In Figure 2, the coordinate of the principal vanishing point is $f\cot\alpha$. When $\alpha = \pi/4$, f = 8 mm, $r_i = f\cot\alpha$ = 8.0000 mm, i.e. $r = r_i$ = 8.0000

Table I.
Offsets in case of $\alpha = +\pi/8$ and $\alpha = -\pi/8$

	ε/μm			ε/μm	
r/mm	$\alpha = \pi/8$	$\alpha = -\pi/8$	r/mm	$\alpha = \pi/8$	$\alpha = -\pi/8$
−20	3.1810	1.5819e-05	20	−1.5819e-05	−3.1810
−15	2.1152	−4.2029e-03	15	4.2029e-03	−2.1152
−10	1.3188	−0.042302	10	0.042302	−1.3188
−8	1.0669	−0.075824	8	0.075824	−1.0669
−5	0.75253	−0.15355	5	0.15355	−0.75253
0	0.37721	−0.37721			

r	a									
	$\pi/20$	$\pi/10$	$3\pi/20$	$\pi/5$	$\pi/4$	$3\pi/10$	$7\pi/20$	$2\pi/5$	$9\pi/20$	$\pi/2$
−18	0.470	1.723	3.968	7.112	10.71	14.105	16.531	17.430	16.589	14.216
−16	0.430	1.492	3.330	5.740	8.431	10.843	12.436	12.834	11.945	9.9875
−14	0.392	1.282	2.716	4.557	6.495	8.126	9.0792	9.1256	8.2588	6.6928
−12	0.357	1.093	2.204	3.549	4.880	5.906	6.3881	6.2101	5.4211	4.2158
−10	0.323	0.923	1.760	2.702	3.558	4.132	4.2890	3.9924	3.3212	2.4402
−8	0.292	0.727	1.380	2.001	2.499	2.754	2.7087	2.3774	1.8483	1.2496
−6	0.263	0.639	1.059	1.434	1.674	1.723	1.5737	1.2698	0.891	0.527
−4	0.236	0.521	0.792	0.985	1.054	0.987	0.810	0.573	0.339	0.156
−2	0.211	0.420	0.575	0.641	0.610	0.498	0.345	0.194	0.081	0.019
0	0.188	0.332	0.401	0.389	0.312	0.205	0.104	0.035	0.004	0.000
2	0.166	0.257	0.266	0.213	0.131	0.058	0.013	4e-04	−9e-04	−0.019
4	0.147	0.195	0.166	0.100	0.039	0.006	6e-07	−0.005	−0.047	−1.562
6	0.128	0.143	0.094	0.0366	4.8e-3	−7e-7	−0.011	−0.078	−0.246	−0.527
8	0.112	0.102	0.047	0.008	0.000	−0.011	−0.092	−0.314	−0.709	−1.245
10	0.097	0.069	0.012	3.0e-4	−0.004	−0.076	−0.319	−0.809	−1.546	−2.440
12	0.0835	0.047	0.005	−2.8e-4	−0.039	−0.247	−0.765	−1.658	−2.871	−4.215
14	0.071	0.026	0.005	−0.007	−0.131	−0.573	−1.503	−2.958	−4.792	−6.692
16	0.060	0.014	−4e-6	−0.036	−0.312	−1.105	−2.607	−4.803	−7.422	−9.987
18	0.05	0.006	−1e-3	−0.099	−0.610	−1.892	−4.151	−7.289	−10.87	−14.21

Table II.
Deviation for different positions with tilt angles (negative values being invalid)

mm, the deviation value is zero. This result is just the deviation value ranging from 0.00 to −0.00 between r = 8 mm and r = 10 mm. Inserting r = fcosα into equation (8) leads to $\varepsilon = 0$.

When r> r_i, the target cannot be imaged in the image plane, and therefore, a negative bias is an invalid solution. Actual job does not appear to make too large photo angle to be measured so that the case does not fall in field of view. There are more than three pixels of the target size requirements besides. In addition, equations (7) and (8) are programmed to be solvable, and the results were completely consistent with the simplification solving symbol code. Inserting $\alpha = 0$ into equation (8), $\varepsilon = 0$ is obtained. Therefore, the deviation equation derivation is correct.

4. Experiments

Experiments were designed to study the distribution of the deviation. Figure 4 shows the setup for the real experiments of the single camera system. The camera captures images from different positions and orientations. The calibration experiment was carried out with Figure 4(a).The circle center deviation experiment was carried out with Figure 4(b).

In the experiment shown in Table II, the radius of the circle was R = 20 mm, focal length f = 15.0 mm and vertical distance from the camera to the target plane H = 1500.0 mm. Figure 5 shows the deviation varying with angle α between the image plane and the circle plane. It appears that the deviation changes slightly slowly when α is less than 0.3 rad, and the deviation is significantly affected with α between 0.4 rad and 0.9 rad. The effect of angle between space and the image plane on the deviation can be seen from Figure 5. The results showed that the photo angle is less than during the change moderate inclination greater than when the error changes steep (Table II and Figure 5). The maximum deviation angle corresponding to the image size, as the amplitude increases, the maximum deviation angle corresponding to increase. As shown in Table II, when r = −12, the maximum deviation corresponds to an inclination of $7\pi/20$, and when r = −14 to −18, the corresponding angle is $2\pi/5$. The maximum deviation changes with the inclination angle with a given image width

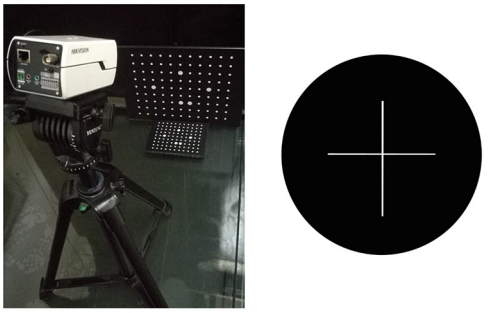

(a) **(b)**

Notes: (a) The calibration template; (b) the original image of the real circle

Figure 4.
Setup for a real experiment of the single-camera system

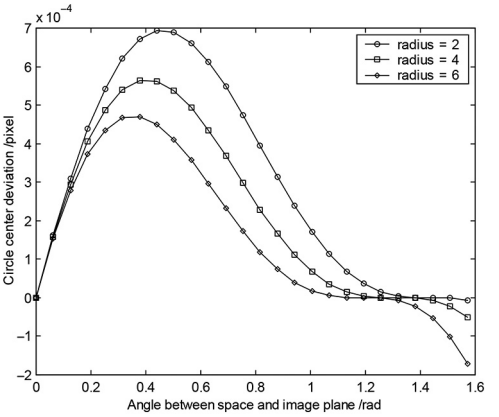

Figure 5.
Deviation ε with tilt angle α

(set maximum radius 6 mm). As seen from Figure 6, when vertical distance H becomes smaller, the maximum deviation angle correspondingly increases.

The influence of radius on the deviation was also investigated. The radius of the circle varied from 2 mm to 19 mm during the experiment, and other parameters were consistent with the above. As can be seen from Figure 7, the deviation increased with the increase in the radius. Seen from Table II, the deviation angle position with the greatest change, 2 mm change in position deviation change $0.18\mu m\pi/4$, the change in position is equivalent to 20 μm deviation change 0.0087 μm. This shows that the deviation of the position change is not very sensitive; also, it shows that the accuracy of measurement of the coordinates of the photograph does not directly affect the calculation of the deviation (too low will affect the value computed of the angle). It can be seen from Table II, that the deviation gradually increases when the tilt angle increases from $3\pi/10$ to $2\pi/5$, and the deviation reaches the maximum 0.266 μm at (r = 2). Thus, the deviation angle change is not very sensitive. In digital photography, it is assumed that a measurement system accuracy of 0.2 μm requires a photo angle measurement accuracy better than $\pm 2°$. This means less precision measurement of the angle of deviation. So there is no iteration solving deviation.

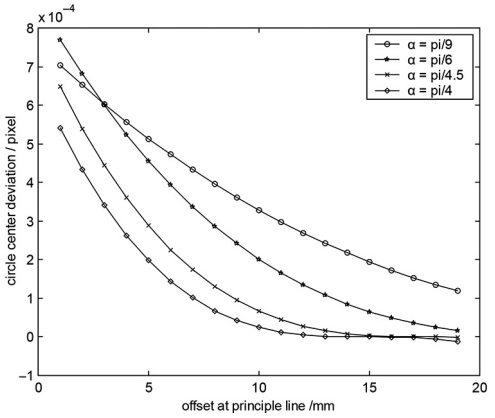

Figure 6.
Deviation variation with position at the principal line

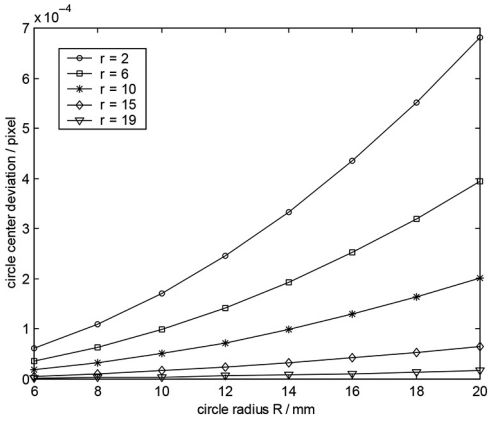

Figure 7.
Deviation variation with the circle radius

5. Conclusion

In the perspective projection model of the camera, the center deviation caused by the space circle projection transformation is analyzed, and then a new algorithm is presented to precisely locate the real projection center of the space circle using projective geometry. I show how to compute the exact 2D projected center coordinate of a circle of known size and construct a projective geometry method and derive simple equations for solving the deviation. Solution distribution of the deviation is also analyzed. The proposed algorithm diminishes a major source of perspective projection error in feature point location and is simple without large iterative computation.

Summarizing the obtained results:

- The direction of the deviation of two centers is pointed to the principal vanishing point, and the deviation is in symmetrical distribution with the symmetry axis of the principal vertical line.
- Maximum deviation occurs at approximately between $3\pi/10$ and $2\pi/5$. The deviation changes slightly slowly when α is less than 0.3 rad, and the deviation is significantly affected with α between 0.4 rad and 0.9 rad.

- The accuracy of measurement of the image coordinates does not directly affect the calculation of the deviation (too low will affect the value computed of the angle).
- The maximum deviation angle corresponding to the image size, as the amplitude increases, the maximum deviation angle corresponding to increase. The deviation increases with increasing radius of the circle.

References

Ahn, S.J. and Rüdiger, K. (1997), "Geometric image measurement errors of circular object targets", *Optical*, Vol. 3, pp. 463-471.

Guillou, E., Meneveaux, D., Maisel, E. and Bouatouch, K. (2000), "Using vanishing points for camera calibration and coarse 3D reconstruction from a single image", *The Visual Computer*, Vol. 16 No. 7, pp. 396-410.

Heikkila, J. (2000), "Geometric camera calibration using circular control points", *IEEE Transactions on Pattern Analysis and Machine Intelligence*, Vol. 22 No. 10, pp. 1066-1077.

Heikkila, J. and Silven, O. (1997), "A four-step camera calibration procedure with implicit image correction", *Proceedings of IEEE Computer Society Conference on Computer Vision and Pattern Recognition, IEEE, San Juan*, Vol. 97.

Huo, J., Guiyang, Z., Jiashan, C. and Ming, Y. (2018), "Corrected calibration algorithm with a fixed constraint relationship and an error compensation technique for a binocular vision measurement system", *Applied Optics*, Vol. 57 No. 19, pp. 5492-5504.

Liu, Z., Wu, Q., Wu, S. and Pan, X. (2017), "Flexible and accurate camera calibration using grid spherical images", *Optics Express*, Vol. 25 No. 13, pp. 15269-15285.

Straub, J., Freifeld, O., Rosman, G., Leonard, J.J. and Fishe, J.W. (2018), "The Manhattan frame model–Manhattan world inference in the space of surface normals", *IEEE Transactions on Pattern Analysis and Machine Intelligence*, Vol. 40 No. 1, pp. 235-249.

Xu, G., Zhang, X., Li, X., Su, J. and Hao, Z. (2016), "Global calibration method of a camera using the constraint of line features and 3d world points", *Measurement Science Review*, Vol. 16 No. 4, pp. 190-196.

Zhl, L., Mei, L. and Yu, S. (2011), "Research on calculation method for the projection of circular target center in photogrammetry", *Chinese Journal of Scientific Instrument*, Vol. 32 No. 10, pp. 2235-2241. In Chinese.

Further reading

Abidi, M.A. and Chandra, T. (1990), "Pose estimation for camera calibration and landmark tracking", *Proceedings of IEEE International Conference on Robotics and Automation, IEEE.*

Almansa, A., Desolneux, A. and Vamech, S. (2003), "Vanishing point detection without any a priori information", *IEEE Transactions on Pattern Analysis and Machine Intelligence*, Vol. 25 No. 4, pp. 502-507.

Andaló, F.A., Taubin, G. and Goldenstein, S. (2015), "Efficient height measurements in single images based on the detection of vanishing points", *Computer Vision and Image Understanding*, Vol. 138, pp. 51-60.

Cui, J-s., Huo, J. and Yang, M. (2015), "The circular mark projection error compensation in camera calibration", *Optik*, Vol. 126 No. 20, pp. 2458-2463.

Cui, J., Huo, J. and Yang, M. (2014), "The high precision positioning algorithm of circular landmark center in visual measurement", *Optik-International Journal for Light and Electron Optics*, Vol. 125 No. 21, pp. 6570-6575.

Liao, X.C. and Feng, W.H. (1999), "Determination of the deviation between the image of a circular", *Journal of Wuhan Technical University of Surveying and Mapping (WTUSM)*, Vol. 24, pp. 235-239. In Chinese.

Oberkampf, D., DeMenthon, D.F. and Davis, L.S. (1996), "Iterative pose estimation using coplanar feature points", *Computer Vision and Image Understanding*, Vol. 63 No. 3, pp. 495-511.

Pătrăucean, V., Gurdjos, P. and Grompone von Gioi, R. (2017), "Joint A contrario ellipse and line detection", *IEEE Transactions on Pattern Analysis and Machine Intelligence*, Vol. 39 No. 4, pp. 788-802.

Penna, M.A. (1991), "Determining camera parameters from the perspective projection of a quadrilateral", *Pattern Recognition*, Vol. 24 No. 6, pp. 533-541.

Shufelt, J.A. (1999), "Performance evaluation and analysis of vanishing point detection techniques", *IEEE Transactions on Pattern Analysis and Machine Intelligence*, Vol. 21 No. 3, pp. 282-288.

Steele, R.M. and Jaynes, C. (2007), "Center-of-mass variation under projective transformation", *Pattern Recognition Letters*, Vol. 28 No. 15, pp. 1915-1925.

Steger, C. (2017), "A comprehensive and versatile camera model for cameras with tilt lenses", *International Journal of Computer Vision*, Vol. 123 No. 2, pp. 121-159.

Wang, J.-G. and Sung, E. (2001), "Pose determination of human faces by using vanishing points", *Pattern Recognition*, Vol. 34 No. 12, pp. 2427-2445.

Yang, W., Fang, B. and Tang, Y.Y. (2018), "Fast and accurate vanishing point detection and its application in inverse perspective mapping of structured road", *IEEE Transactions on Systems, Man, and Cybernetics: Systems*, Vol. 48 No. 5, pp. 755-766.

Zhang, G. and Wei, Z. (2003), "A position-distortion model of ellipse centre for perspective projection", *Measurement Science and Technology*, Vol. 14 No. 8, p. 1420.

Corresponding author
Yu Sun can be contacted at: 785100001@qq.com